electronic structure in different environments.

The Relationship between Structural Transferability and Energy Additivity

Transferability has often been used to rationalize observations of additivity.[16] For example, Rothenberg[31] has shown that orbitals of methane and ethane can be localized and that one-electron properties of the localized C–H orbitals vary by less than 2–3%. The kinetic energy associated with a C–H orbital in methane is 0.8690 au while the corresponding quantity for ethane in the staggered conformation is 0.886 au.[31] These values are within 2% of each other, but the difference corresponds to about 10 kcal. However, additivity holds to a much higher degree for unbranched saturated hydrocarbons. For example, the total energies[28,32a] of propane (−118.09211 au), ethane (79.11582 au), and methane (−40.13978 au) are additive to within 0.08 kcal (4-31 G basis set). This additivity is not appreciably dependent on basis set and is seen for minimum basis sets as well.[28,32b] This comparison suggests that the degree of transferability seen with localized orbitals is not sufficient to account for the additivity in total energy.

In a similar vein, Degand, Leroy, and Peeters[33] have reproduced orbital energies for methane, ethane, and propane to within 0.1% by transferring Fock matrix elements derived from a basis set of localized orbitals. This comparison emphasizes that transferability is a reasonable description of the total wave functions, but the degree of additivity differs from the corresponding ab initio calculation by over 30 kcal.[33b]

Another method based on transferable Fock matrix elements is the SAMO technique[34a] which has been applied to ethane, propane, and butane. The direct ab initio calculation gives additive total energies to within 0.10 kcal, while the SAMO energies are only additive to 30 kcal.[34b]

Conclusions

In the previous paper,[12] it was demonstrated analytically that energy additivity does not require wave function transferability or constant electronic structure. In the current paper, examples have been presented which show a high degree of additivity in total energy, but not because of constant electronic structure. Large positive kinetic energy deviations ($\sim$80 kcal) in one spatial region are offset by comparable negative deviations in other regions to give a total kinetic energy which is additive to 0.1 kcal. The present work has shifted the focus from group transferability to mutual cancelation as the root of energy additivity.

(31) S. Rothenberg, *J. Am. Chem. Soc.*, **93**, 68 (1971).

(32) (a) L. Radom, W. J. Hehre, and J. A. Pople, *J. Am. Chem. Soc.*, **94**, 2371 (1972). (b) The 3G energies of methane, ethane, and propane are −39.72686, −78.30618, and −116.88580 au (L. Radom and J. A. Pople, *ibid.*, **92**, 4786 (1970)). The additivity is within 0.10 kcal.

(33) (a) Ph. Degand, G. Leroy, and D. Peeters, *Theor. Chim. Acta*, **30**, 243 (1973). (b) The ab initio orbital energies for methane, ethane, and propane are −28.3284, −55.3636, and −82.5678 au. The orbital energy of ethane is 53.02 kcal above the mean orbital energy of methane and propane. In the same basis set (ref 33a), the transferable matrix element procedure gives −28.3000, −55.37980, and −82.5210 au. The absolute values agree reasonably well, but the orbital energy for "transferable" ethane is only 19.26 kcal above the mean.

(34) (a) J. E. Eilers and D. R. Whitman, *J. Am. Chem. Soc.*, **95**, 2067 (1973). (b) The ab initio energies of ethane, propane, and butane are −78.8196, −117.6776, and −156.5353 au. The corresponding SAMO energies are −78.8049, −117.6275, and −156.5479 au.

Catecholate and Phenolate Iron Complexes as Models for the Dioxygenases

Robert H. Heistand II, Randall B. Lauffer, Erol Fikrig, and Lawrence Que, Jr.*

Contribution from the Department of Chemistry, Baker Laboratory, Cornell University, Ithaca, New York 14853. Received September 28, 1981

Abstract: The syntheses and physical properties of a series of Fe(salen)X and Fe(saloph)X complexes where X is phenolate or catecholate are reported. Magnetic susceptibility measurements as well as electronic, infrared, and NMR spectra indicate that the catecholate in Fe(salen)catH behaves very much like a phenolate and is concluded to be monodentate in its coordination to the iron. The abstraction of a proton from Fe(salen)catH results in an anionic complex, [Fe(salen)cat]⁻, with markedly different properties; the catecholate in this complex is chelated. Both monodentate and chelated catecholate complexes are high-spin ferric, demonstrating that catecholate coordination to a bis(phenolato)iron(III) complex does not result in the reduction of the ferric center. This is in agreement with observations made on dioxygenase–substrate complexes. In addition, studies on a series of Fe(salen)X complexes where X is phenolate, thiophenolate, benzoate, and catecholate show that the dominant salen-to-Fe(III) charge-transfer interaction is modulated by the coordination of these ligands. Comparisons with corresponding dioxygenase complexes show that the tyrosinate-to-iron(III) charge-transfer interactions are similarly affected, thus indicating that the salen ligand provides a reasonable approximation of the iron environment in the dioxygenases.

The interaction of molecular oxygen with metalloenzymes is currently an area of considerable activity.[1] One interesting reaction is the dioxygenation of catechols to yield *cis,cis*-muconic acids, catalyzed by the nonheme iron enzymes catechol 1,2-dioxygenase and protocatechuate 3,4-dioxygenase.[2,3] Spectroscopic studies on these enzymes show the active site iron to be a mo-

(1) Hayaishi, O., Ed. "Molecular Mechanisms of Oxygen Activation"; Academic Press: New York, 1974.

(2) Nozaki, M., in ref 1, Chapter 4.

(3) Que, L., Jr. *Struct. Bonding (Berlin)* **1980**, *40*, 39–72.

nonuclear high-spin ferric center[4,5] coordinated to at least two tyrosines.[6,7] The nature of the other ligands as well as the coordination number of the iron is not currently established. The tyrosinate coordination gives rise to a ligand-to-metal charge-transfer interaction resulting in the red color observed for these enzymes.[6-9] The binding of substrate and inhibitors to the enzymes alters their absorption spectra, resulting in striking color changes which range from yellow to purple.[6,7,10,11] Resonance Raman studies on these complexes show that the tyrosines are not displaced upon binding of substrate or inhibitors.[6,7,12]

On the basis of the spectroscopic studies of the dioxygenases, we have initiated efforts to mimic the coordination environment of the active-site iron with inorganic complexes. We have briefly reported the synthesis of a monodentate catecholate iron complex which serves as a model of the enzyme–substrate complex.[13] The rationale for a monodentate catechol complex arises from steady-state inhibition kinetic experiments on protocatechuate 3,4-dioxygenase with hydroxybenzoate inhibitors,[14] which suggest that the enzyme exhibits a preference for binding the *p*-OH. Resonance Raman studies[7] have subsequently confirmed the coordination of the phenolate to the iron in the *p*-hydroxybenzoate complex and the absence of such an interaction in the *m*-hydroxybenzoate complex. These observations thus suggest that the substrate may be bound in a monodentate fashion in the enzyme–substrate complex. A crystal structure of one such model complex,[15] Fe(saloph)catH,[17] as well as the reaction of a related complex with oxygen,[16] has been published. In this paper, we report the syntheses of a series of catecholate and phenolate complexes and the characterization of their properties in the solid state and in solution. We also compare these synthetic complexes to their corresponding dioxygenase complexes.

Experimental Section

Synthesis. The commercially available reagents were purified as follows: sublimation at reduced pressure—resorcinol, 4-chlororesorcinol, catechol, 4-*tert*-butylcatechol, 3-methylcatechol, hydroquinone, phenol, *p*-chlorophenol, 2,4,6-trichlorophenol, *p*-cyanophenol, and *p*-cresol; distillation at reduced pressure—*o*-methoxyphenol, *o*-chlorophenol, *m*-fluorophenol, *o*-phenylenediamine, and *o*-bromophenol; recrystallization—3,5-di-*tert*-butylcatechol from *n*-heptane and 18-crown-6 according to literature procedures.[18] Tetrahydrofuran was distilled under N_2 from potassium benzophenone. Reagent acetonitrile (Burdick and Jackson) was trap-to-trap distilled from NaH under reduced pressure. Methylene chloride was distilled under N_2 first from

P_2O_5 and then from K_2CO_3 (baked at 230 °C under vacuum) and stored over activated 3-Å sieves. Potassium hydride was washed with THF to remove the mineral oil and stored under N_2. All other reagents were used without further purification.

Starting Metal Complexes. [Fe(salen)]$_2$O and [Fe(saloph)]$_2$O were synthesized according to published procedures.[19] Anhydrous basic ferric acetate[20a,b] was used in a modified literature procedure to make Fe(salen)OAc,[19b] Fe(saloph)OAc,[20b] and Fe(5-Cl-salen)OAc.

General Procedure for Iron Phenolate Complexes. All manipulations were performed in a Schlenk apparatus under N_2 or Ar atmospheres scrubbed of O_2 and H_2O. A degassed saturated solution of the acetate complex in acetonitrile was heated to reflux and filtered. To the hot filtrate was added a degassed solution of the phenolic compound. Slow cooling induced crystallization. The product was collected by vacuum filtration and washed with ethyl acetate. Reagent acetonitrile was used for the syntheses of salen complexes, but dry acetonitrile was necessary for the syntheses of saloph complexes. The following compounds were synthesized by using this procedure: Fe(salen)catH,[13] Fe(salen)4-NO$_2$catH,[13] Fe(salen)DBcatH,[16] Fe(salen)3-Me-catH, Fe(salen)4-Me-catH, Fe(5-Cl-salen)catH, Fe(salen)(OPh-2-F) Fe(salen)(OPh-2-Cl)8, Fe(salen)(OPh-2-Br), [Fe(salen)]$_2$hq,[15] Fe(saloph)catH,[15] Fe(saloph)4-Cl-resH, Fe(saloph)(OPh-2-F), Fe(saloph)(OPh-2-Cl), and Fe(saloph)(OPh-2-Br). All compounds obtained were crystalline and afforded satisfactory elemental analyses. For further details, consult ref 21.

K$^+$[Fe(salen)cat]$^-$·0.75(18-Crown-6)·THF. All operations were performed in a drybox. Potassium *tert*-butoxide (0.330 g, 2.9 mmol), 18-crown-6 (0.670 g, 2.5 mmol), and freshly pulverized Fe(salen)catH (1.04 g, 2.4 mmol) were mixed as solids. Dry acetonitrile (13 mL) was added to the mixture, generating a green solution that was filtered into a flask containing 100 mL of dry THF. The filter was washed with THF and the volume of solution raised to 230 mL. Five days later the K$^+$[Fe(salen)cat]$^-$ was isolated as black 2-mm cubes (0.44 g, 25%). Recrystallization was achieved by dissolving 0.60 g in 4 mL of CH$_3$CN, filtering into 70 mL of THF, and washing with 10 mL of THF. Two days later small black crystals (0.40 g, 67%) were isolated. Gas chromatography, mass spectroscopy, NMR spectroscopy, and single-crystal X-ray diffraction studies[21] support the formulation of the solid as stated above. Anal. Calcd for C$_{35}$H$_{44}$FeKN$_2$O$_{9.5}$: C, 56.83; H, 6.00; Fe, 7.55; K, 5.29; N, 3.79. Found: C, 56.72; H, 6.03; Fe, 7.74; K, 5.00; N, 4.08.

Deuterated Compounds. Catechol was converted to C$_6$H$_4$(OD)$_2$ by dissolving 2 g in 10 mL of D$_2$O, lyophilizing the D$_2$O, and repeating with 10 mL more of D$_2$O. 3-Methylcatechol was deuterated by heating an anaerobic solution in D$_2$O (20 mL, 0.44 M) with potassium *tert*-butoxide (0.40 M) in a sealed tube at 170 °C for 20 h. Rapid quenching with acid, ether extraction, evaporation of solvent, and sublimation produced 3-methyl-4,5,6-trideuteriocatechol.

Physical Measurements. Solid-state magnetic susceptibilities were measured over the range 1.9–300 K by using the Faraday method with Spectrosil quartz buckets and Cahn electrobalance force recording as described elsewhere.[22a] Measurements were recorded at five different fields (3.6–11.8 kG), but no field dependence was observed for the calculated value of the coupling constant *J*. Diamagnetic corrections were calculated from Pascal's constants, and the data analysis program[22b] was based on literature methods.[22c] Calibration was achieved with the HgCo(SCN)$_4$ standard. Solution magnetic susceptibilities were obtained by the Evans method[23a] on a Varian EM390 NMR spectrometer, and the appropriate solvent, density, and diamagnetic corrections were appplied.[23b] The susceptibilities of Fe(salen)BcatH, Fe(salen)(OPh-2-Cl) and Fe(salen)(OPh-2-Br) were determined on solutions generated from 10 mM [Fe(salen)]$_2$O in CH$_2$Cl$_2$ with 3% Me$_4$Si by the addition of the appropriate amount of axial ligand sufficient for 99.9% complexation (vide infra). The measurements of the [Fe(salen)cat]$^-$ anion were made on solutions generated by reaction of KH with Fe(salen)catH in THF (4 mM) and by dissolving the crystalline complex in CH$_3$CN (10 mM).

Optical spectra were recorded on a Cary 219 UV–visible spectrophotometer. Solution and solid-state infrared spectra were taken on Per-

(4) Que, L., Jr.; Lipscomb, J. D.; Zimmermann, R.; Munck, E.; Orme-Johnson, W. H.; Orme-Johnson, N. R. *Biochim. Biophys. Acta* **1976**, *452*, 320–334.

(5) Kent, T.; Munck, E.; Widom, J.; Que, L., Jr., unpublished results.

(6) Que, L., Jr.; Heistand, R. H., II; Mayer, R.; Roe, A. L. *Biochemistry* **1980**, *19*, 2588–2593.

(7) Que, L., Jr.; Epstein, R. M. *Biochemistry* **1981**, *20*, 2545–2549.

(8) Tatsuno, Y.; Saeki, Y.; Iwaki, M.; Yagi, T.; Nozaki, M.; Kitagawa, T.; Otsuka, S. *J. Am. Chem. Soc.* **1978**, *100*, 4614–4615.

(9) Keyes, W. E.; Loehr, T. M.; Taylor, M. L. *Biochem. Biophys. Res. Commun.* **1978**, *83*, 941–945.

(10) Fujisawa, H.; Uyeda, M.; Kojima, J.; Nozaki, M.; Hayaishi, O. *J. Biol. Chem.* **1972**, *247*, 4414–4421.

(11) Kojima, Y.; Fujisawa, H.; Nakazawa, A.; Nakazawa, T.; Kanetsuna, F.; Taniuchi, H.; Nozaki, M.; Hayaishi, O. *J. Biol. Chem.* **1967**, *242*, 3270–3278.

(12) Felton, R. H.; Cheung, L. D.; Phillips, R. S.; May, S. W. *Biochem. Biophys. Res. Commun.* **1978**, *85*, 844–850.

(13) Que, L., Jr.; Heistand, R. H., II. *J. Am. Chem. Soc.* **1979**, *101*, 2219–2221.

(14) Que, L., Jr.; Lipscomb, J. D.; Munck, E.; Wood, J. M. *Biochim. Biophys. Acta* **1977**, *485*, 60–74.

(15) Heistand, R. H., II; Roe, A. L.; Que, L., Jr. *Inorg. Chem.* **1982**, *21*, 676–681.

(16) Lauffer, R. B.; Heistand, R. H., II, Que, L., Jr. *J. Am. Chem. Soc.* **1981**, *103*, 3947–3949.

(17) Abbreviations used: saloph, *o*-phenylenebis(salicyclideneimine) dianion; catH$_2$, catechol; salen, ethylenebis(salicyclideneimine) dianion; OAc, acetate; hqH$_2$, hydroquinone; DBcatH$_2$, 3,5-di-*tert*-butylcatechol; 3-Me-catH$_2$, 3-methylcatechol; 4-Me-catH$_2$, 4-methylcatechol; 4-Cl-resH, 4-chlororesorcinol; DPIXDME, deuteroporphyrin dimethyl ester dianion; DBSQ, 3,5-di-*tert*-butyl-*o*-semiquinone anion.

(18) Valentine, J. S. In "Biochemical and Clinical Aspects of Oxygen"; Caughey, W. S., Ed.; Academic Press: New York, 1979; pp 659–677.

(19) (a) Lewis, J.; Mabbs, F. E.; Richards, A. *J. Chem. Soc. A* **1967**, 1014–1018. (b) Pfeiffer, P.; Breith, E.; Lübbe, E.; Tsumaki, T. *Liebigs Ann. Chem.* **1933**, *503*, 84–130.

(20) (a) Hardt, V. H. D.; Möller, W. *Z. Anorg. Allg. Chem.* **1961**, *313*, 57–69. (b) Koch, S.; Holm, R. H.; Frankel, R. B. *J. Am. Chem. Soc.* **1975**, *97*, 6714–6723. (c) Lewis, J.; Mabbs, F. E.; Richards, A.; Thornley, A. S. *J. Chem. Soc. A* **1969**, 1993–1997.

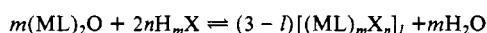(21) Heistand, R. H., II. Ph.D. Thesis, Cornell University, 1982.

(22) (a) Young, J. E., Jr. Ph.D. Thesis, Cornell University, 1971. (b) Scott, C., Cornell University, 1979. (c) Bevington, P. R. "Data Reduction and Error Analysis for Physical Sciences"; McGraw-Hill: New York, 1969.

(23) (a) Evans, D. F. *J. Chem. Soc.* **1959**, 2003–2005. (b) Binstead, R. A.; Beattie, J. K.; Dewey, T. G.; Turner, D. H. *J. Am. Chem. Soc.* **1980**, *102*, 6442–6451.

Catecholate and Phenolate Iron Complexes

J. Am. Chem. Soc., Vol. 104, No. 10, 1982 2791

kin-Elmer 299B and Perkin-Elmer 337 grating infrared spectrophotometers. Gas chromatograms were obtained on a Perkin-Elmer Sigma 3 gas chromatograph. Mass spectral analyses were determined by the Cornell mass spectroscopy facility. Paramagnetic ^{1}H NMR spectra were run on a Bruker WM300 spectrometer.

Titration Studies. All solutions were either made at 25 °C or corrected to 25 °C for density-dependent concentration changes. All measurements were run on a Cary 219 spectrophotometer thermostated to 25.0 ± 0.1 °C with a Neslab RTE-4 refrigerated circulating bath. Aerobic titrations were made by repetitively adding 2–10-μL aliquots of the phenol solution to a stoppered 1-cm cuvette containing 5.00 mL of an oxo-bridged dimer solution in dried CH_2Cl_2 (~3×10^{-4} M in Fe). The solution was stirred magnetically for 15 min prior to recording a measurement. The total concentration was corrected for the slight dilution from the added ligand. Anaerobic titrations were obtained for catechol and hydroquinone by making a separate solution in the drybox for each data point. Data was collected at 380 and 492 nm for Fe(salen)OAc, at 450, 416, and 370 nm for Fe(salen)phenolate, catecholate, resorcinolate, and hydroquinone, and at 520 and 372 nm for all Fe(saloph)X complexes.

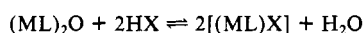**Analysis.** There are three possibilities for the structure of the Fe-(salen)phenolate complexes in solution. The first is the solid-state dimer [Fe(salen)X]$_2$, the second is a monomer Fe(salen)X, and the third possibility which exists for dihydroxybenzenes is [Fe(salen)]$_2$X. A general equation which encompasses the formation of all three structures from [Fe(salen)]$_2$O and the phenol is given as follows:
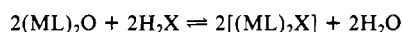
$$m(ML)_2O + 2nH_mX \rightleftharpoons (3 - l)[(ML)_mX_n]_l + mH_2O$$

Case I: $m = n = 1, l = 2$

$$(ML)_2O + 2HX \rightleftharpoons [(ML)X]_2 + H_2O$$

Case II: $m = n = l = 1$

$$(ML)_2O + 2HX \rightleftharpoons 2[(ML)X] + H_2O$$

Case III: $m = 2, n = l = 1$

$$2(ML)_2O + 2H_2X \rightleftharpoons 2[(ML)_2X] + 2H_2O$$

Thus, the equilibrium constant for all cases is defined as

$$K = \frac{[[(ML)_mX_n]_l]^{3-l}[H_2O]^m}{[(ML)_2O]^m[H_mX]^{2n}}$$

A general linear equation is obtained for this system by following the derivation outlined by Momoki et al.[24a] and using his nomenclature for a linear plotting method of curved molar ratio titrations:

$$\chi/\kappa_i = a + b[H_2O]^{m/2n}\kappa_i^{[(3-l)/2n]-1}(1 - \kappa_i)^{-m/2n}$$

$$a = n/m$$

$$b = (1/2)^{-m/2n}K^{-1/2n}m^{(l-3)/2n}l^{(l-3)/2n}C_m^{(3-l-m-2n)/2n}$$

where C_m = total concentration of metal ion (not (ML)$_2$O), C_l = total concentration ligand, $\chi = C_l/C_m$, K = formation constant, and κ_i = % complexation for a given $\chi_i = [(A_s)_i - (A_s)_m]/[(A_s)_{max} - (A_s)_m]$, where $(A_s)_i$ = absorbance for a given χ_i, $(A_s)_m$ = initial absorbance of metal species, and $(A_s)_{max}$ = absorbance at complete complexation.

A graph of χ/κ_i vs. $f(\kappa_i)$ will only be linear when the correct values of l, m, and n are chosen. For example: Case I: $m = n = 1, l = 2$

$$\chi/\kappa_i = a + b[H_2O]^{1/2}\kappa_i^{-1/2}(1 - \kappa_i)^{-1/2}$$

$$a = 1, b = K^{-1/2}C_m^{-1}$$

Case II: $m = n = l = 1$

$$\chi/\kappa_i = a + b[H_2O]^{1/2}(1 - \kappa_i)^{-1/2}$$

$$a = 1, b = (1/2KC_m)^{-1/2}$$

Case III:[25] $m = 2, n = l = 1$

$$\chi/\kappa_i = a + b[H_2O](1 - \kappa_i)^{-1}$$

$$a = 1/2, b = K^{-1/2}C_m^{-1}$$

Therefore all three cases can be identified because all have a different $f(\kappa_i)$ necessary to obtain a linear graph. The only case we have observed to date is case II.

In order to obtain K from the slope, the concentration of water must be known. This was determined by the method of standard additions where the reciprocal of the conditional formation constant ($[H_2O]/K$) of Fe(salen)OAc was plotted vs. the added $[H_2O]$. The slope of the resulting line is K^{-1} and the intercept $[H_2O]_{residual}K^{-1}$. During these titrations the $[H_2O]$ could be assumed to be constant since the $[H_2O]$ was always more than an order of magnitude greater than the $[(ML)_2O]$. Also for cases I and II, the water term contributes as the square root. For subsequent batches of solvent, a titration of Fe(salen)OAc would calibrate the residual water.

For better determination of the formation constants, a computer nonlinear least-squares analysis program[24b] based on literature derivations[24c] was used for a two-parameter fit where both constants K and $(A_s)_{max}$ were determined. The changing $[H_2O]$ was also included. In all cases $(A_s)_{max}$ was within 1% of the experimental values, and attempts to fit the titrations to either case I or III would result in ridiculous values for $(A_s)_{max}$.

Enzyme Studies. Catechol 1,2-dioxygenase (E.C. 1.13.11.1) was prepared from *Pseudomonas arvilla* C-1 (ATCC 23974) according to literature procedures.[26] Steady-state inhibition kinetic experiments were performed in 50 mM potassium phosphate buffer, pH 7.5, at 25 °C on a Gilson K-1C oxygraph. Substrate and inhibitor were premixed with the enzyme addition last. K_i values were obtained from Lineweaver–Burk and Dixon plots. All inhibitors studied were found to be competitive. In some cases, K_D values were also obtained from spectrophotometric titrations of enzyme with inhibitors; these values were in agreement with K_i values.

Results and Discussion

Synthesis. The design of synthetic models for the active sites of the iron dioxygenases is understandably at a very rudimentary stage due to the paucity of information on the iron coordination. The tetradentate ligands, salen and saloph, have been chosen for

salen

saloph
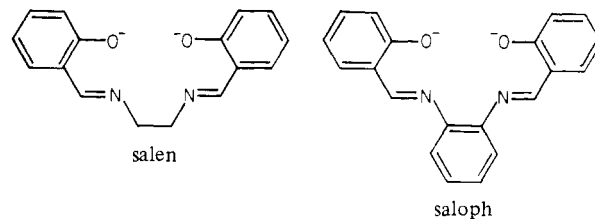
two reasons. Firstly, the preference of these ligands for a planar geometry[27] in many metal complexes may hinder the chelation of catechol and thus afford a complex with a monodentate catecholate ligand. Secondly, the phenolate moieties mimic the two tyrosinate coordination of the iron in the dioxygenases[6,7] while the imine functionalities provide some correspondence with the postulated imidazole binding[4] in the enzymes. Thus, the spectral properties of the various complexes synthesized based on these ligand systems may be compared with those of corresponding enzyme complexes.

The best synthetic procedure involves the use of the acetate complexes in a ligand exchange reaction with excess phenols, catechols, resorcinols, or hydroquinones.

$$Fe(salen)OAc + nHOC_6H_4X \xrightarrow[n = 3–30]{CH_3CN} Fe(salen)(OC_6H_4X)$$
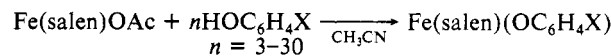
The acetates were preferable to the μ-oxo dimers as starting material because of the greater solubilities of the former compounds. The catechol complexes require the least excess ligand to drive the reaction; the amount of excess phenol required varies greatly and depends on the acidity of the phenol. This excess ligand is needed to displace the generally better binding acetate and prevent hydrolysis of the resultant complexes by trace amounts of water in the solvent to yield the more stable μ-oxo dimers (vide infra). All complexes synthesized are microcrystalline to crystalline, frequently of X-ray quality, with colors ranging from bronze to green and from maroon to black.

(24) (a) Momoki, K.; Sekino, J.; Sato, H.; Yamaguchi, N. *Anal. Chem.* **1969**, *41*, 1286–1299. (b) Wilcox, C. F., Cornell University, 1977. (c) Wentworth, W. E. *J. Chem. Educ.* **1965**, *42*, 96–103.

(25) This is the general case derived by Momoki et al.[24a] where A + B ⇌ C + D. The resulting equation differs by the square root of K since case III is defining the square of the formation constant.

(26) Fujiwara, M.; Golovleva, L. A.; Saeki, Y.; Nozaki, M.; Hayaishi, O. *J. Biol. Chem.* **1975**, *250*, 4848–4855.

(27) Murray, K. S. *Coord. Chem. Rev.* **1974**, *12*, 1–35.

2792 *J. Am. Chem. Soc., Vol. 104, No. 10, 1982*

Heistand et al.

Table I. Magnetic Susceptibility Data

compounds	μ_{eff}/Fe, μ_B	T, K	J, cm^{-1}	ref
Faraday Method Measurements				
Fe(saloph)catH	5.92 ± 0.03	4–300		*a*
	(θ = 1.1 ± 0.1)			
Fe(saloph)(OPh-2-Cl)	5.88 ± 0.03	294		*a*
Fe(saloph)(4-Cl-resH)	5.88 ± 0.02	294		*a*
Fe(saloph)tfa	5.54	301	−5.0	31
Fe(salen)catH	5.51 ± 0.03	293	−5.1 ± 0.1	*a*
Fe(salen)(OPh-2-Br)	5.52 ± 0.03	298	−4.1 ± 0.1	*a*
Fe(salen)(OPh-2-Cl)	5.54 ± 0.02	294		*a*
Fe(salen)[OPh-2,4,6-(NO$_2$)$_3$]	5.66	270	−4.5 ± 0.5	29
Fe(salen)Cl	5.35 ± 0.5	299	−7.5 ± 0.6	31
Fe(salen)tfa	5.7 ± 0.1	270	−6.3 ± 0.3	29
[Fe(salen)]$_2$Cl$_4$cat	5.44	286	−0.65	30
[Fe(salen)]$_2$hq	5.32	286	−2.5	30
[Fe(salen)]$_2$O	1.87	295	−95	27
Evans Method Measurements				
Fe(salen)BcatH^b	5.91 ± 0.04	307		*a*
Fe(salen)(OPh-2-Br)	5.88 ± 0.04	307		*a*
Fe(salen)(OPh-2-Cl)	5.88 ± 0.04	307		*a*
[Fe(salen)cat]$^-$	5.85 ± 0.1	307		*a*

^{a} This work. ^{b} 4-*tert*-Butylcatecholate complex was used for solubility reasons.

The syntheses of complexes of other dihydroxybenzenes have also been explored. Previously the [Fe(salen)]$_2$hq complex was synthesized by oxidative addition of *p*-benzoquinone to Fe(salen).[28] Our ligand exchange method with hydroquinone produces the same binuclear iron complex with a 2:1 metal-to-ligand stoichiometry,[15] in contrast to the monodentate catechol complexes, which exhibit 1:1 metal-to-ligand stoichiometry. To complete the series, we have also obtained a resorcinol complex with a stoichiometry similar to that of the catecholate complexes.

An anionic form of Fe(salen)catH can be obtained by treatment of the complex with KH or potassium *tert*-butoxide. Large well-defined crystals are obtained when 18-crown-6 is added to a THF solution of K$^+$[Fe(salen)cat]$^-$, and an X-ray crystallographic study is in progress.[21] On the basis of the elemental analyses, density measurements (1.34 g/mL) and the ongoing X-ray diffraction study, the crystals are best formulated as K$^+$[Fe(salen)cat]$^-$·0.75(18-crown-6)·THF. Gas chromatography and mass spectrometry confirm the presence of the crown ether and the solvent in the crystals.

Solid-State Studies. The crystal structure of Fe(saloph)catH, showing a monodentate catecholate complex, has been reported.[15] For further elucidation of the structures of the other newly synthesized complexes, variable-temperature magnetic susceptibility measurements from 1.9 to 300 K were carried out on selected complexes and room temperature measurements were made on others. The results are listed in Table I. For the saloph series, all complexes studied are consistent with a high-spin d^5 configuration.

The situation is quite different for the Fe(salen)X complexes. The temperature dependences of the magnetic susceptibility and the magnetic moment of Fe(salen)catH and Fe(salen)(OPh-2-Br) (Figure 1 and Tables II and III) show the presence of Néel points and suggest antiferromagnetic interactions. This is not unusual for Fe(salen)X complexes, however. For ferric dimers, the antiferromagnetic coupling interaction has been described,[27,29] and values for the coupling constant J can be obtained by a computer fit of the data. Both Fe(salen)catH and Fe(salen)(OPh-2-Br) exhibit J values in the range of 4–5 cm^{-1}. Such J values are consistent with a structure, exemplified by [Fe(salen)Cl]$_2$, which exhibits a J of −7.5 cm^{-1}.[31] The X-ray crystal structure of the
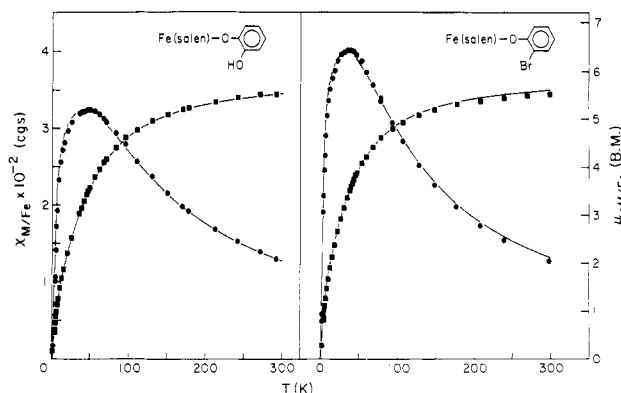

Figure 1. Variable-temperature magnetic susceptibility at a field strength of 11.8 kG. The experimental magnetic susceptibility and effective magnetic moments are represented by circles and squares, respectively. The solid line is the least-squares two-parameter fit (g and J) to the Heisenberg, Dirac, and van Vleck equation.[27,29] The g and J values are respectively 2.015 and −5.08 cm^{-1} for Fe(salen)catH and 2.010 and −4.09 cm^{-1} for Fe(salen)(OPh-2-Br).

chloro dimer[32] shows the antiferromagnetic interaction arising from the stacking of one Fe(salen)Cl moiety above the other such that a salicylyl hydroxyl of one acts as a distal ligand to the other in the dimer. Thus coupling occurs through a di-μ-aryloxy bridge. Other Fe(salen)X complexes with −J values of 4.5–7.0 cm^{-1} include complexes where X = trichloroacetate, salicylate, phenylacetate, and picrate.[29,31] These complexes have also been assumed to have the [Fe(salen)Cl]$_2$ structure. Such a structure for [Fe(salen)-catH]$_2$ would have one catecholate oxygen replacing the Cl, leaving the other oxygen as a free hydroxyl. Thus the catecholate ligand in [Fe(salen)catH]$_2$ is monodentate as well.

The infrared spectra of several catecholate complexes obtained in Nujol mulls also corroborate the monodentate catecholate structure. Sharp ν_{OH} stretches are observed for Fe(salen)catH, Fe(5-Cl-salen)catH, and Fe(salen)DBcatH at 3380, 3378, and 3383 cm^{-1}, respectively ($\Delta\nu$ at half-height 23, 17, and 13 cm^{-1}, respectively). For Fe(salen)catD, the ν_{OH} shifts to 2520 cm^{-1} (calculated, 2460 cm^{-1}). For Fe(saloph)catH and Fe(saloph)4-Cl-resH, the ν_{OH} appears as a broad band centered near 3200 cm^{-1}, indicative of hydrogen bonding. This conclusion is corroborated in the crystal structure of Fe(saloph)catH.[15]

Solution Studies. The solution properties of the Fe(salen) and Fe(saloph) complexes are somewhat different from those in the solid. Initial Evans' susceptibility measurements[23] on these complexes revealed anomalously low values for the solution magnetic moments, and electronic spectra of the complexes also differed from spectra obtained in the presence of excess ligand. It was subsequently realized that these complexes were susceptible to hydrolysis from trace amounts of water in the solvent; the hydrolysis resulted in the formation of the μ-oxo dimer, i.e.,

$$2Fe(salen)X + H_2O \rightleftharpoons [Fe(salen)]_2O + 2HX$$
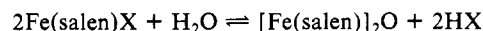
The extent of hydrolysis appeared dependent on the nature of the axial ligand, and this prompted a study of the formation constants for these complexes.

The formation constant for this system is defined by

$$K = \frac{[Fe(salen)X]^2[H_2O]}{[[Fe(salen)]_2O][HX]^2}$$

The approach chosen to determine the values of K was a linear plotting adaptation of the molar ratio method developed by Momoki et al.[24a] A graphical solution was obtained first and then refined by a nonlinear least-squares regression.[24b,c] This method enables us to determine the amount of residual water in the dried

(28) Floriani, C.; Fachinetti, G.; Calderazzo, F. *J. Chem. Soc., Dalton Trans.* **1973**, *765*–769.

(29) Wollmann, R. G.; Hendrickson, D. N. *Inorg. Chem.* **1978**, *17*, 926–930.

(30) Kessel, S. L.; Hendrickson, D. N. *Inorg. Chem.* **1978**, *17*, 2630–2635. Kessel, S. L.; Emberson, R. M.; Debrunner, P. G.; Hendrickson, D. N. *Inorg. Chem.* **1980**, *19*, 1170–1178.

(31) Gerloch, M.; Lewis, J.; Mabbs, F. E.; Richards, A. *J. Chem. Soc. A* **1968**, 112–116. Lewis, J.; Mabbs, F. E.; Richards, A.; Thornley, A. S. *J. Chem. Soc. A* **1969**, 1993–1997.

(32) Gerloch, M.; Mabbs, F. E. *J. Chem. Soc. A* **1967**, 1900–1908.

Table IV. Formation Constants and Spectral Data for Iron Complexes

HX	$pK_a{}^a$	Fe(salen)X			Fe(saloph)X		
		$\log K^b$	λ_{max}, nm	ϵ, $10^3 M^{-1}$ cm^{-1} ^{c}	$\log K^b$	λ_{max}, nm	ϵ, $10^3 M^{-1}$ cm^{-1} ^{c}
acetic acid	4.76	3.49	492, 316	4.85, 11.26	2.16	365	16.4
2,4,6-trichlorophenol	7.42	3.25	428	7.05			
p-cyanophenol	7.95	3.16	426	7.58	2.66	375	17.4
o-chlorophenol	8.48	0.95	418	7.24			
m-fluorophenol	9.28	1.12	415	7.30			
p-chlorophenol	9.38	1.41	416	7.33	1.12	373	16.7
resorcinol	9.42^d	1.39	412	7.15			
catechol	9.45^d	3.84 ± 0.2	418	6.77	3.43	371	16.9
hydroquinone	9.85^d	1.29	407	6.77			
o-methoxyphenol	9.98	−1.40	417	6.31			
p-cresol	10.26	0.28	410	7.11	0.00	367^e	16.7

^{a} Values obtained from ref 33. ^{b} Error in log K is ±0.1. ^{c} Error in extinction coefficient is ±0.5%. ^{d} First dissociation constant. ^{e} Shoulder.
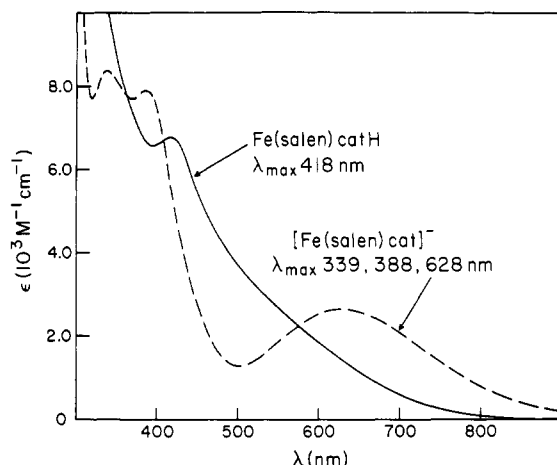
Figure 2. Optical spectra of Fe(salen)catH in CH$_2$Cl$_2$ (solid line) generated anaerobically from [Fe(salen)]$_2$O with 4.4 equiv of catechol and K$^+$[Fe(salen)cat]$^-$ (dashed line) generated anaerobically in THF from Fe(salen)catH by the addition of KH.

solvent as well as the point of 100% complexation. We also establish that Fe(salen)X is a monomer in solution (cf. Analysis). This conclusion is consistent with Evans' susceptibility measurements[23] obtained in solutions having ligand concentrations sufficiently in excess to ensure complete formation of the complexes (Table I). In all cases studied, the Fe(salen)X complexes are in the high-spin ferric state with no antiferromagnetic interactions.

Table IV lists the formation constants for the complexes studied, together with their absorbance maxima and extinction coefficients. The formation constants span 5 orders of magnitude and depend on the acidity of the phenol. A graph of the pK_a of the phenol vs. the logarithm of the formation constant for the corresponding Fe(salen) complex is shown in Figure 2. There is clearly a linear correlation of pK_a vs. log K for the meta- and para-substituted phenols, indicating that the formation of the phenolate complex from the μ-oxo dimer may be thought of as an acid–base reaction with the phenol acting as acid and the dimer as base. Ortho-substituted phenols, not unexpectedly, exhibit a steric effect resulting in lower formation constants, though a linear correlation persists within the ortho-substituted subgroup. Catechol, however, is an exception; it exhibits very high affinity for [Fe(salen)]$^+$, approximately 3 times higher than acetate.

The formation constants for five Fe(saloph)X complexes have also been measured (Table IV). The three para-substituted phenol complexes exhibit a linear correlation between the pK_a of the phenol and the formation constant of the complex, just like the Fe(salen)X complexes. Catecholate again exhibits a higher than expected affinity for [Fe(saloph)]$^+$. In general, however, the affinity of X$^-$ for [Fe(saloph)]$^+$ is less than that for [Fe(salen)]$^+$.

Our studies also include the hydroquinone complex of Fe(salen)$^+$. The iron-to-hydroquinone stoichiometry of crystals derived from either the Floriani synthesis[28] or the ligand exchange

method[15] is clearly 2:1, and a crystal structure of this complex shows the hydroquinone bridging two Fe(salen) moieties.[15] In solution, however, the titration studies unequivocally determine the stoichiometry to be 1:1, i.e., hydroquinone behaves like a phenol. NMR studies (vide infra) confirm this with the observation of appropriately shifted ortho and meta hydroquinone proton resonances. On the basis of the available information, we have suggested that the 2:1 stoichiometry in the crystal is a result of crystallization.[15]

The higher affinity of the catecholate (catH$^-$) ligand for the iron in these complexes is quite interesting but somewhat puzzling. At first glance, this higher affinity may be attributed to a secondary interaction between the ferric center and the other catecholate oxygen. (*o*-Methoxyphenol, for example, has been found to act as a bidentate ligand in several complexes.[34]) However, our solid-state data provide no evidence for this secondary interaction. Furthermore, the similarity of the electronic and NMR (vide infra) spectra of the catH$^-$ complexes to those of the phenolate complexes indicates this interaction, if present at all, is quite weak and thus insufficient to account for the formation constants observed.

We have also considered the possibility of an intermolecular hydrogen bonding interaction between the catecholate O–H and a nucleophilic site on salen to stabilize the catecholate complex. This is not unreasonable in view of the intermolecular hydrogen bond between the catecholate O–H and a saloph O in the neighboring molecule observed in the Fe(saloph)catH structure.[15] Solution IR studies on Fe(salen)catH (2 mM in CH$_2$Cl$_2$) reveal the presence of a ν_{OH} at 3481 cm^{-1}, which is broader ($\Delta\nu_{1/2}$ 50 cm^{-1}) than that observed in Nujol mulls but at higher energy. Hydrogen-bonding interactions should have lowered the ν_{OH} rather than increased it. A second ν_{OH} is observed at 3560 cm^{-1}, which matches both the position and intensity of the expected amount of free catechol in solution.

A comparison of the crystal structures[15] of Fe(saloph)catH and [Fe(salen)]$_2$hq perhaps provides an answer. The Fe–O$_{axial}$ bond in the former complex is 1.828 Å, compared to 1.861 Å in the latter complex—a 0.03-Å contraction. The catecholate thus appears to form a stronger Fe–O bond, and this results in a more stable complex.

Fe(salen)catH exhibits a visible spectrum (Figure 3) with an absorbance maximum at 418 nm, typical of all other phenolate complexes. The spectrum results from both salen-to-iron and catecholate-to-iron charge-transfer interactions, but these are not clearly resolved. In contrast, [Fe(salen)cat]$^-$ exhibits a visible

(33) pK_as of phenols obtained from the following: Korüm, G.; Vogel, W.; Andrussow, K. *Pure Appl. Chem.* **1961**, *1*, 190–536. Oae, S.; Price, C. C. *J. Am. Chem. Soc.* **1958**, *80*, 4938–4941. Cook, A. H. Bunbary, H. M.; Hey, D. H. "Dictionary of Organic Compounds"; Oxford University Press: New York, 1965.

(34) Bullock, J. I.; Hobson, R. J.; Povey, D. C. *J. Chem. Soc., Dalton Trans.* **1974**, 2037–2043. Bullock, J. I.; Ladd, M. F. C.; Povey, D. C. *J. Chem. Soc., Dalton Trans.* **1977**, 2242–2246. Greenhough, T. J.; Ladd, M. F. C. *Acta Crystallogr., Sect., B* **1978**, *B34*, 2744–2752.

Table V. Chemical Shifts in Fe(salen)X Complexes[a]

X	solvent	salen shifts, δ				X shifts, δ
		3-H	4-H	5-H	6-H	
Cl⁻	CDCl₃	84	-80	70	-50	
OAc⁻	CDCl₃	83	-78	69	-48	Me -144[b]
OBz⁻	CDCl₃	84	-79	70	-48	m-H -12
SPh⁻	acetone-d₆	76	-76	69	-50	o-H 76; m-H -57; p-H 79
SPh-4-Me⁻	acetone-d₆	76	-75	65	-50	o-H 76; m-H -58; p-Me -95
OPh⁻	acetone-d₆	66	-70	52	-42	o,p-H 94; m-H -87
OPh-3,5-Me₂⁻	acetone-d₆	66	-70	52	-42	o,p-H 96; m-Me 31
OPh-4-Me⁻	acetone-d₆	66	-70	51	-42	o-H 101; m-H -89; p-Me -110
OPh-2,5-Me₂⁻	acetone-d₆	66	-70	51	-42	o-Me -84; m-H -102; m-Me -32; p-H 102
OPh-4-OH⁻(hqH⁻)	acetone-d₆	64	-69	50	-41	o-H 110; m-H -85
3-Me-catH⁻ ᶜ	acetone-d₆	67	-71, -69	50, 53	-42, -40	3-Me -89, 28; m-H -91; o,p-H 94, 104
4-Me-catH⁻ ᶜ	acetone-d₆	68	-71	53	-42	4-Me -109, 27; o,p-H 98; m-H -95, -98
cat²⁻	acetone-d₆	43	-57	34	-27	3,6-H 14; 4,5-H -10
3-Me-cat²⁻	acetone-d₆	42	-56	32	-25	3-Me -32; 4,5-H -23; 6-H 8
4-Me-cat²⁻	acetone-d₆	41	-56	32	-25	4-Me -47; 3,6-H 8, 18
DBcat²⁻	acetone-d₆	40	-54	31	-25	4-H -18

[a] ¹H NMR spectra were obtained on a Brucker WM-300 NMR spectrometer operating in the FT mode at 300 K. All shifts are relative to Me₄Si, with downfield shifts negative. [b] Reference 35. [c] Two isomers depending on which catechol oxygen coordinates to the iron. Catechol ring protons are assigned relative to the catechol oxygen coordinated to the metal.
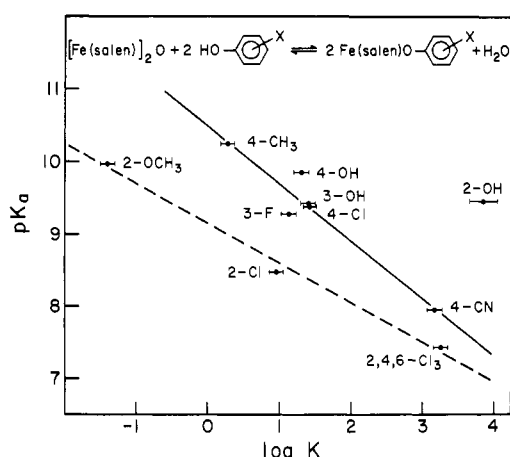
Figure 3. Graph of the aqueous pKₐs of substituted phenols vs. the log of their formation constants for complexation with [Fe(salen)]₂O determined in CH₂Cl₂ at 25 °C.

spectrum with λₘₐₓ at 339, 388, and 628 nm (Figure 3). The 628-nm band has been assigned to the catecholate-to-iron charge-transfer interaction,[16] and the 388-nm band arises presumably from the salen-to-iron interaction, shifted to higher energy due to the chelation of the catecholate. The corresponding DBcat²⁻ complex can also be generated by the reduction of Fe(salen)DBSQ with superoxide.[16] X-ray crystallographic studies in progress indicate that the catecholate is chelated in [Fe(salen)cat]⁻, in agreement with spectroscopic and electrochemical studies in solution.[16] Evans's susceptibility measurements on the complex are consistent with a high-spin ferric center, though the magnetic moment obtained is slightly lower than the spin-only value. We attribute this to slight decomposition of the complex in solution. Unlike the other complexes we have studied where excess ligand is added to ensure complete formation of the complexes, excess catecholate dianion cannot be added to a solution of [Fe(salen)cat]⁻, for this results in the formation of [Fe(cat)₃]³⁻.

NMR Spectra. The ¹H NMR spectra of these complexes provide further characterization. Due to the high-spin ferric center and, in many cases, relatively short electron spin–lattice relaxation times, large isotropic shifts of up to 100 ppm are observed for the various proton resonances, leading to well-resolved spectra (Table V). Resonances due to the salen ligand are assigned by analogy to those of previously studied Fe(salen)OAc.[35] The magnitude of the shifts, however, depends considerably on the nature of the

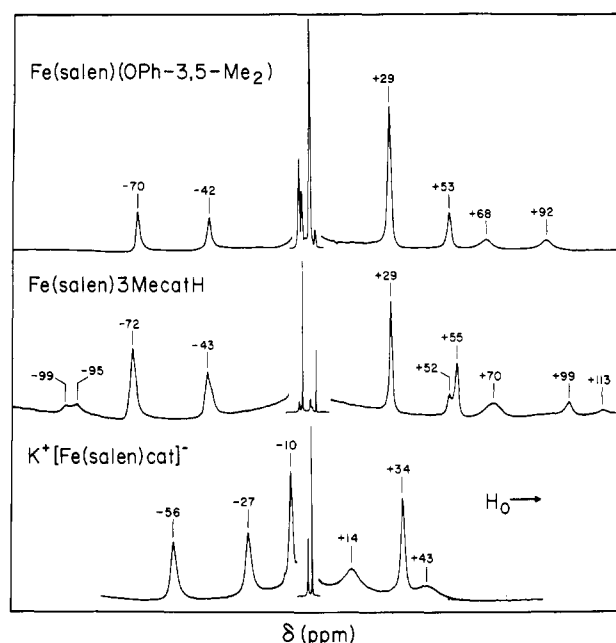Figure 4. 300-MHz ¹H NMR spectra of (A) Fe(salen)(OPh-3,5-Me₂) in CD₂Cl₂, (B) Fe(salen)3-Me-catH in CD₂Cl₂, and (C) K⁺[Fe(salen)-cat]⁻·0.75(18-crown-6)·THF in acetone-d⁶. These spectra exhibit resonances in the diamagnetic region due to (A) a 20-fold excess of 3,5-dimethylphenol and (B) a 1-fold excess of 3-methylcatechol.

axial ligand. For example, about 160 ppm separates the most downfield-shifted and the most upfield-shifted salen resonances in the carboxylate and halide complexes, while the separation is only 140 ppm in the phenolate complexes and 100 ppm in the chelated catecholate complexes.

Representative 300-MHz ¹H NMR spectra of these complexes, shown in Figure 4, illustrate the similarity of the salen shifts for the phenolate and 3-Me-catH complexes, consistent with the monodentate structure suggested for the latter complex. In addition, isotropically shifted resonances from the axial phenolate are observed (not previously reported at 80 MHz).[16] The phenolate complex exhibits resonances at 94 and -87 ppm, assigned by methyl substitution to the 2,4,6 and 3,5 phenolate protons, respectively, in agreement with assignments for Fe(DPIXDME)OPh.[36] This alternating shift pattern, also seen for the salicylaldimine protons, is indicative of π delocalization of

(35) LaMar, G. N.; Eaton, G. R.; Holm, R. H.; Walker, F. A. J. Am. Chem. Soc. 1973, 95, 63–75.

(36) Caughey, W. S.; Johnson, L. F. J. Chem. Soc., Chem. Commun. 1969, 1362–1363.

unpaired spin density and dominant contact interactions.[37]

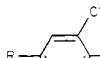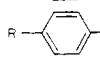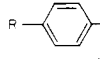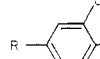Similarly, paramagnetically shifted resonances are observed for the axial ligand in Fe(salen)3-Me-catH. The resonance at +29 ppm assigned to the methyl group identifies the major component of the solution as the complex wherein the O-1 oxygen of the catechol is bound to the iron (O-1 isomer). This assignment is confirmed by the use of ring-deuterated 3-Me-catH$_2$. There is also a methyl resonance at −98 ppm corresponding to the O-2 isomer. Other resonances are assigned to the catecholate protons by analogy to those of the phenolate complexes (Table V). Fe-(salen)4-Me-catH also exhibits two sets of resonances in acetone-d_6, corresponding to the O-1 and O-2 isomers, and the resonances can be assigned as with the 3-Me-catH$^-$ complex. The similarity of the catecholate shifts to the phenolate shifts thus corroborates the suggested monodentate ligation of the catH$^-$ ligand to [Fe(salen)]$^+$ in solution. Finally, studies in CDCl$_3$ CD$_2$Cl$_2$, and acetone show that the O-1 and O-2 isomers in each complex interconvert on the NMR time scale, the isomerization being fastest in CDCl$_3$. Further studies on the dynamics of these systems are in progress.

The NMR spectra of the [Fe(salen)cat]$^-$ complexes are quite different from those of their parent Fe(salen)catH compounds. We have earlier reported the absence of any NMR resonances for [Fe(salen)DBcat]$^-$ in CDCl$_3$ at 80 MHz.[16] At 300 MHz, however, broad salen resonances are observed that are more than 3 times as broad as those of phenolate complexes, i.e., (2000 Hz for the 4-H salen peak compared to 520 Hz in the 3,5-di-methylphenolate complex). The lines are much sharper in acetone-d_6 (Figure 4), and both salen and catecholate resonances are observed. There are only two catecholate resonances, assigned to 3,6 (14 ppm) and 4,5 (−10 ppm) protons, consistent with the chelated structure.

The much smaller catecholate isotropic shifts compared to those of the phenolates indicate the presence of two opposing spin-polarization pathways. With a chelated catecholate structure, spin can be polarized through both oxygens. The catecholate protons, however, are related differently to each oxygen. H-3, for example, is ortho to O-2 and meta to O-1. Thus, spin polarization through O-1 would result in a chemical shift of ca. −90 ppm, while the same through O-2 would give a resonance at ca. +100 ppm. The effect of having both pathways operative is a much reduced isotropic shift, as is observed. The observed methyl shifts further illustrate the dual spin-polarization pathways; both 3-methyl and 4-methyl shifts are downfield and much larger than corresponding proton shifts. Table V shows that the shift of a m-Me group (+30 ppm) in a phenol is considerably smaller than the shift of either an o-Me or a p-Me group ($\sim$−100 ppm). In the chelated catecholate complexes, the methyl groups will always be meta to one oxygen and ortho or para to the other, with the latter determining the sign of the shift—thus, the observed downfield methyl shifts.[38]

Relevance to the Dioxygenases. We have synthesized phenolate and catecholate iron complexes and characterized their physical properties in the solid state and in solution. Magnetic susceptibility measurements on Fe(salen)catH and [Fe(salen)cat]$^-$ show both complexes to be high-spin ferric; i.e.,the catecholates do not reduce the iron upon binding, which is in agreement with Mössbauer studies on the dioxygenase–substrate complexes.[4,5] These observations are also consistent with electrochemical studies on ferric catecholate complexes,[39] which show a stabilization of the ferric oxidation state relative to the ferrous state upon catecholate coordination. This stabilization is, however, contrary to mechanisms proposed earlier wherein the substrate reduces the ferric center

(37) Horrocks, W. D., Jr. In "NMR of Paramagnetic Molecules. Principles and Applications"; LaMar, G. N., Horrocks, W. D., Jr., Holm, R. H., Eds.; Academic Press: New York, 1973; Chapter 4.

(38) Similar arguments can be used to assign the catecholate resonances in the NMR spectrum of the cluster complex [MoFe$_4$S$_4$(SC$_2$H$_5$)$_3$-(C$_6$H$_4$O$_2$)$_3$]$^{3-}$. Wolff, T. E.; Berg, J. M.; Holm, R. H. *Inorg. Chem.* **1981**, *20*, 174–180.

(39) Avdeef, A.; Sofen, S. R.; Bregante, T. L.; Raymond, K. N. *J. Chem. Soc.* **1978**, *100*, 5362–5370. Harris, W. B.; Carrano, C. J.; Copper, S. R.; Sofen, S. R.; Avdeef, A. E.; McArdle, J. V.; Raymond, K. N. *J. Am. Chem. Soc.* **1979**, *101*, 6097–6104.

Table VI. Comparison of the Electronic Spectra of Fe(salen)X with Corresponding Dioxygenase Complexes

	Fe(salen)X (R = H)	CTD-X^a (R = H)	PCD-X^b (R = COO$^-$)
H$_2$O		455	460
R—⟨⟩—O$^-$ (Cl)	418	440	420
R—⟨⟩—S$^-$	380, 440	385, 470	
R—⟨⟩—COO$^-$	492	505	525
R—⟨⟩—O$^-$ (OH)	418		
		465, ~680^c	475, ~690^c
R—⟨⟩—O$^-$ (O$^-$)	339, 388, 628		

^{a} Catechol 1,2-dioxygenase data obtained from ref 6. ^{b} Protocatechuate 3,4-dioxygenase data obtained from ref 7. ^{c} Catecholate-to-iron(III) charge-transfer interaction approximated from ES vs. E difference spectrum.
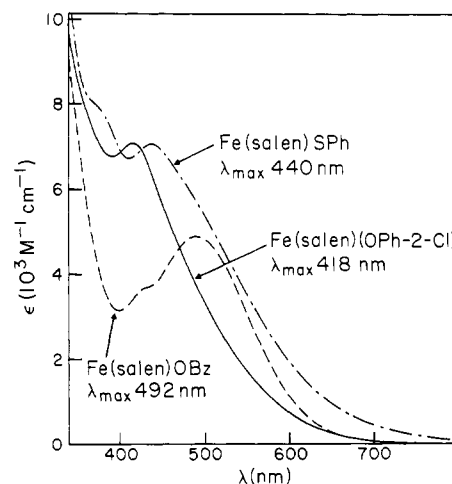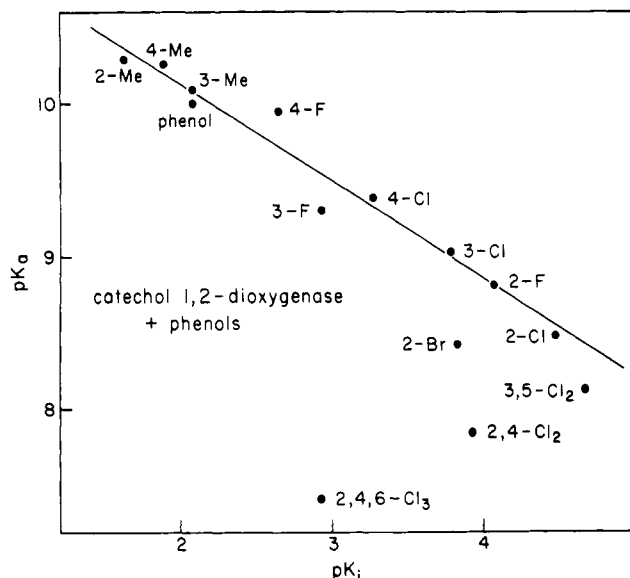

Figure 5. Optical spectra of Fe(salen) o-chlorophenolate, thiophenolate, or benzoate generated in CH$_2$Cl$_2$ from [Fe(salen)]$_2$O by the addition of 43, 140, and 19 equiv of o-chlorophenol, thiophenol, and benzoic acid, respectively. The Fe(salen)SPh solution was anerobic.

to the ferrous oxidation state, rendering the iron capable of binding oxygen.[11] Instead, we have suggested an alternative mechanism[14] whereinthe iron center activates the substrate for oxygen attack. Indeed, we have recently observed that Fe(salen)DBcatH reacts readily with oxygen to yield the semiquinone complex, Fe(salen)DBSQ[16]—the initial step in our proposed mechanism. In contrast, [Fe(salen)DBcat]$^-$ is unreactive with oxygen.[16] The reactivity studies would thus imply a monodentate coordination for the substrate. Comparisons of the visible spectra of the two catecholate complexes with those of the ES complexes do not provide a definitive answer at present (Table VI), so the question of whether the substrate catechol is monodentate or chelated in its coordination to the active site iron in the dioxygenases remains to be resolved.

Comparisons of the visible spectra of the dioxygenase inhibitor complexes with those of corresponding Fe(salen)X complexes, however, are more informative (Table VI). Resonance Raman studies of the enzyme complexes[6,7] show that the tyrosinate-to-iron charge-transfer interaction is modulated by the binding of various ligands. Similar changes are observed in the salen-to-iron interaction in the synthetic complexes (Figure 5). Though the maxima observed in the models are clearly blue-shifted with respect to those of the enzyme complexes, the order of increasing energy is retained. This correlation is remarkable considering the simplicity of the model system. Unfortunately, we have been

Figure 6. Graph of the aqueous pK_as of substituted phenols vs. pK_is obtained from steady-state inhibition kinetic studies on catechol 1,2-dioxygenase.

unable to include a model for the native enzyme in this series, because water is thought to be the ligand displaced by the exogenous ligands in the inhibitor complexes.[14,41] As discussed earlier, [Fe(salen)H$_2$O]$^+$ has not been synthesized because of the much greater stability of the μ-oxo dimer.

The affinities of a series of phenols for catechol 1,2-dioxygenase can also be compared with the formation constants of the Fe(salen)OPh series. Figure 6 shows the results of our steady-state kinetic study, which indicates that the more acidic phenols are the better inhibitors.[42] Exceptions to the linear correlation can be rationalized by using steric arguments. Thus, like the model complexes, acid–base chemistry is a significant factor in the

(40) LaMar, G. N.; Walker, F. A. *J. Am. Chem. Soc.* **1973**, *95*, 6950–6956.

(41) Lipscomb, J. D.; Whittaker, J. W.; Arciero, D. M. In "Oxygenases and Oxygen Metabolism"; Nozaki, M., Ishimura, Y., Yamamoto, S., Coon, M. J., Ernster, L., Estabrook, R. W., Eds.; Academic Press: Tokyo, in press.

(42) A similar correlation was obtained in a study of another catechol 1,2-dioxygenase and its affinity for substituted catechols. Dorn, E.; Knackmuss, H.-J. *Biochem. J.* **1978**, *174*, 85–94.

formation of the enzyme complexes. Also interesting is the observation that ortho-substituted phenols fall on the same line as their meta and para isomers in the enzyme study, while the ortho-substituted phenols are clearly less strongly bound in the model study. This difference suggests that the iron site in the enzyme may be less sterically hindered than in Fe(salen)X and that certain geometries (e.g., octahedral) may be considered less likely possibilities for the iron environment in the dioxygenases.

In summary, we have characterized a series of Fe(salen)X complexes whose physicochemical and spectroscopic properties provide us with a greater understanding of the iron environment in the catechol dioxygenases. Current work is aimed at the development of ligand systems that will more closely mimic the properties of the ferric complex in these enzymes.

Supplementary Material Available: Tables II and III listing magnetic susceptibility data for Fe(salen)catH and Fe(salen)(OPh-2-Br), respectively (2 pages). Ordering information is given on any current masthead page.